Research Paper
Computational Methods for Differential Equations
http://cmde.tabrizu.ac.ir
Vol. *, No. *, *, pp. 1-15
DOI:10.22034/cmde.2026.72411.3657

Iterative solution methods for time-fractional nonlinear Volterra integro-differential equations in ecological models

Siba Prasad Mohapatra[1], **Shubham Yadav**[2], **Anasuya Nath**[3], **Jugal Mohapatra**[2,*]

[1]Department of Mathematics, Konark Institute of Science and Technology, India.

[2]Department of Mathematics, National Institute of Technology Rourkela, India.

[3]Department of Mathematics, Utkal University, Bhubaneswar,India.

Abstract

This study proposes and investigates a finite difference method, built on an iterative framework, for numerically solving a nonlinear fractional integro-differential equation of Volterra type that models population dynamics within an isolated system. The model incorporates a time-fractional derivative of Caputo type with order $\alpha \in (0,1)$. To approximate this operator, the scheme utilizes the L1 discretization on a uniformly spaced grid, and the integral component is evaluated using the composite trapezoidal rule. At each time level the resulting nonlinear algebraic equation is a scalar quadratic equation, which is solved through the Daftardar–Gejji and Jafari iterative approach. The rigorous convergence analysis establishes an order of convergence of $2-\alpha$ for sufficiently smooth solutions. The accuracy of the scheme is demonstrated through several computational examples, including a solution with a weak initial singularity and a comparison with results available in the literature for Volterra's population model.

Keywords. Fractional Volterra type model, Fractional integro-differential equation, L1 scheme, Trapezoidal rule, Error estimation.
2010 Mathematics Subject Classification. 26A33, 45J05, 65R20, 45D05.

Uncorrected Proof

1. Introduction

Fractional calculus extends the principles of classical calculus by allowing differentiation and integration to be defined for arbitrary, non-integer orders. This generalization provides a powerful and adaptable framework for addressing complex problems across various fields, including science, engineering, and applied mathematics. Originating in the late 17^{th} century, fractional calculus has recently attracted substantial interest for its wide-ranging applications, spanning areas such as physics, engineering, and financial modeling. The strength of fractional calculus stems from its capability to capture memory effects and hereditary characteristics in dynamic systems. In contrast to classical integer-order models—where the system's current behavior is influenced solely by its present input—fractional derivatives incorporate the cumulative influence of past states. This feature makes fractional models particularly suitable for describing phenomena such as anomalous diffusion, viscoelastic responses, and other systems governed by non-local dynamics. For further discussion, see [1, 22, 26] and references therein. Analyzing population dynamics plays a vital role in fields such as ecology, biology, and resource management. Mathematical modeling serves as a key tool in exploring how populations evolve, reach equilibrium, or diminish in response to environmental pressures and biological interactions. In 1971, Scudo [20] introduced a nonlinear Volterra-type model to describe the growth of a species in an isolated environment. This formulation incorporates intrinsic reproduction rates, effects of population density, and memory-dependent behavior resulting from the influence of historical population levels, given by:

Received: 13 May 2026; Accepted: 14 November 2026.
∗ Corresponding author. Email: jugal@nitrkl.ac.in.

$$\begin{cases} \dfrac{d}{dt}z(t) = a(t)z(t) - bz^2(t) - \lambda z(t)\displaystyle\int_0^t z(s)\,ds, \quad t \in (0,T], \\ z(0) = z_0, \end{cases} \tag{1.1}$$

where $T \in \mathbb{R}^+$. Here, the function $z(t)$ represents the population size at time t, while $a(t)$ is a time-dependent intrinsic growth rate that may vary due to environmental factors, and the term $a(t)z(t)$ represents the natural growth of the population. The parameter $b > 0$ accounts for density-dependent competition, which limits growth as population size increases. The quadratic term $(-bz^2(t))$ accounts for intra-species competition. The integral term introduces a memory effect, where $\lambda > 0$ represents the strength of suppression due to the accumulated past population. This term implies that the population at time t is affected by the cumulative past population size, possibly modeling long-term resource depletion or delayed density-dependent effects, which are common in closed ecological systems. Finally, z_0 represents an initial population size.

This work focuses on a time-fractional population growth model represented as a nonlinear Volterra-type integro-differential equation (FVIDE), formulated as follows:

$$\begin{cases} \mathcal{D}_t^\alpha z(t) = a(t)z(t) - bz^2(t) - \lambda z(t)\int_0^t z(s)ds + f(t), \quad t \in (0,T], \\ z(0) = z_0, \end{cases} \tag{1.2}$$

Here, $\mathcal{D}_t^\alpha$ represents the Caputo fractional derivative of order α. To simplify the formulation, we incorporate a source function $f(t)$. The inclusion of a fractional-order derivative alongside an integral term introduces nonlocal behavior, while the presence of both quadratic and integral nonlinearities sets this model apart from traditional growth models such as the logistic or Gompertz types. Due to the inherent nonlocality and strong nonlinearity, finding exact analytical solutions is generally infeasible, thereby necessitating the use of numerical methods for detailed analysis. Over recent decades, significant progress has been made in constructing semi-analytical and numerical methods to approximate solutions of intricate population growth models like (1.2). As an example, Xu [27] utilized the homotopy analysis method to obtain an approximate analytical solution, representing the solution as a polynomial series. In [16], Parand and co-authors developed two numerical techniques based on the collocation method, employing Sinc and Rational Legendre basis functions to address Volterra's population model (1.1). Later, Marzban et al. [11] introduced a hybrid numerical strategy that combines block-pulse functions with Lagrange interpolation polynomials to approximate the solution of (1.1). Maleki and Kajani [10] proposed a multi-domain Legendre–Gauss pseudospectral technique to compute approximate solutions for (1.2). Furthermore, in [17], Parand and Delkhosh employed a collocation approach using generalized fractional-order Chebyshev orthogonal functions of the first kind to handle the same population growth model (1.2). A fractional shifted Legendre polynomial-based scheme was proposed in [7] to solve (1.2), where the authors also provided a detailed convergence study along with corresponding error estimates. Baleanu et al. [2] employed the fuzzy transform technique to address the model (1.2), notably without imposing limitations on the number of discretization points within the problem domain. In [21], proposed an innovative collocation framework that utilizes Gegenbauer wavelets in conjunction with the quasi-linearization method to approximate solutions of the fractional-order population growth model within a closed environment. To facilitate this approach, operational matrices for fractional integration were constructed using block-pulse functions, and the quasi-linearization strategy was employed to effectively manage the resulting nonlinear algebraic system.

Volterra-type integral and integro-differential equations have also been treated by many other numerical techniques. For instance, Legendre wavelets were used for two-dimensional fractional integro-differential equations in [15], and a computational method for two-dimensional linear Volterra integral equations of the first kind was proposed in [23]. A class of nonlinear Volterra integro-differential equations was solved numerically in [19], and a convergence analysis of a collocation method for two-dimensional fractional Volterra integro-differential equations was given in [5]. Collocation methods based on Fibonacci polynomials [13], a matrix approach based on novel operational matrices [12], and moving least squares combined with spectral collocation for stochastic Volterra integro-differential equations [14] are further examples.

Uncorrected Proof

The motivation for the present work is twofold. From the modelling viewpoint, Volterra's model describes a species living in a closed environment whose growth is limited both by crowding (the quadratic term) and by the accumulated toxic effect of its own past population (the integral term). Replacing the first derivative by a Caputo derivative of order $\alpha \in (0,1)$ introduces a power-law memory into the growth rate, which is appropriate for populations with hereditary effects. The resulting model (1.2) contains a nonlocal derivative together with a quadratic and an integral nonlinearity, so closed-form solutions are not available and reliable numerical solvers are needed. From the computational viewpoint, most of the solvers cited above for this model [2, 7, 10, 11, 16, 17, 21, 27] are global methods that turn the problem into a coupled nonlinear algebraic system, which is then solved by Newton-type or quasi-linearization iterations. In contrast, the scheme proposed here is a time-marching scheme: at every time level the unknown solves only a scalar quadratic equation, which the DGJ iteration handles in a few explicit steps. It is proved to converge in the maximum norm with order $(2-\alpha)$ (Theorem 4.3). Its limitations, in particular for solutions with a weak singularity at $t=0$, are discussed in Remark 5.5 and illustrated in Section 5.

Inspired by the aforementioned studies, the present work investigates the qualitative characteristics of the model's solutions, emphasizing numerical simulations to demonstrate various population growth patterns. The L1 method discretizes the fractional derivative by applying piecewise linear interpolation over each subinterval to estimate the unknown function. The integral term is evaluated using the composite trapezoidal rule. The system of nonlinear algebraic equations resulting from the discretization is solved via the Daftardar–Gejji and Jafari (DGJ) iterative scheme. A convergence study, carried out under the discrete maximum norm, provides an error estimate and confirms that the method attains a convergence order of $(2-\alpha)$. To support the theoretical findings, numerical experiments are carried out, complemented by tabulated data and graphical representations. These results highlight the accuracy and reliability of the proposed method. The outcomes of this investigation hold potential applications in ecological modeling, formulating conservation strategies, and managing resources within isolated environments. The structure of the paper is as follows: Section 2 outlines the necessary preliminaries and introduces the Daftardar–Gejji and Jafari (DGJ) method. In Section 3, the numerical discretization of Equation (1.2) over a uniform grid is detailed. Section 4 is devoted to the analysis of error bounds and the convergence behavior of the scheme. Section 5 presents numerical examples, including a weakly singular solution, a study of the computational cost, and a comparison with results from the literature, that corroborate the theoretical predictions. Lastly, Section 6 summarizes the key conclusions of the study. Let $\mathcal{C}(\Omega)$ denote the space of continuous real-valued functions defined on the domain Ω. The symbol $\|\cdot\|_\infty$ is used to represent the maximum (or uniform) norm. The constant C is employed generically across various inequalities, where its value may differ from one instance to another.

Uncorrected Proof

2. Preliminaries

2.1. **Basic fractional calculus.** The subsequent definitions and fundamental properties are essential for the analysis presented in this study. For a more comprehensive treatment, the reader is referred to [18].

Definition 2.1. The Riemann–Liouville fractional integral of order $\widetilde{\alpha} \in \mathbb{R}^+$ for a function $\varphi(x) \in \mathcal{C}[a,b]$ is given by:

$$J_x^{\widetilde{\alpha}}\varphi(x) = \frac{1}{\Gamma(\widetilde{\alpha})}\int_a^x (x-s)^{\widetilde{\alpha}-1}\varphi(s)\,ds.$$

$\Gamma(\cdot)$ is gamma function.

Definition 2.2. For a function $\varphi(x) \in \mathcal{C}^m[a,b]$, the Caputo fractional derivative of order $\widetilde{\alpha} \in \mathbb{R}^+$ is expressed as:

$$\mathcal{D}_x^{\widetilde{\alpha}}\varphi(x) = J_x^{m-\widetilde{\alpha}}\varphi^{(m)}(x) = \begin{cases} \dfrac{1}{\Gamma(m-\widetilde{\alpha})}\displaystyle\int_a^x (x-s)^{m-\widetilde{\alpha}-1}\varphi^{(m)}(s)\,ds, & \text{if } \widetilde{\alpha} \in (m-1,m), \\ \varphi^{(m)}(x), & \text{if } \widetilde{\alpha} = m, \end{cases}$$

where $m-1 < \widetilde{\alpha} \le m$.

Definition 2.3. The Mittag-Leffler function involving two positive parameters β and γ is formulated as follows:

$$E_{\beta,\gamma}(w) = \sum_{k=0}^{\infty} \frac{w^k}{\Gamma(\beta k+\gamma)}, \qquad w \in \mathbb{C}.$$

Some properties of fractional derivative are as follows:

(1) Linearity: Let ϵ_1, ϵ_2 be positive constants, then

$$J_x^{\widetilde{\beta}}\{\epsilon_1\,\eta_1(x) \pm \epsilon_2\,\eta_2(x)\} = \epsilon_1 J_x^{\widetilde{\beta}}\eta_1(x) \pm \epsilon_2 J_x^{\widetilde{\beta}}\eta_2(x),$$

$$\mathcal{D}_x^{\widetilde{\beta}}\{\epsilon_1\,\eta_1(x) \pm \epsilon_2\,\eta_2(x)\} = \epsilon_1 \mathcal{D}_x^{\widetilde{\beta}}\eta_1(x) \pm \epsilon_2 \mathcal{D}_x^{\widetilde{\beta}}\eta_2(x).$$

(2) For $x \in [a,b]$, $J_x^{\widetilde{\beta}}\mathcal{D}_x^{\widetilde{\beta}}\varphi(x) = \varphi(x) - \sum_{j=0}^{m-1} \varphi^{(j)}(a)\frac{(x-a)^j}{\Gamma(j+1)}$, $\widetilde{\beta} \in (m-1, m)$.

2.2. **DGJ method.** In [3], Daftardar–Gejji and Jafari introduced a novel iterative decomposition technique for solving nonlinear functional equations of the form:

$$u = \eta + \mathcal{F}(u), \tag{2.1}$$

where η is a known function and $\mathcal{F}$ is a nonlinear operator. The method assumes that the solution u can be expressed as an infinite series:

$$u = \sum_{n=0}^{\infty} u_n. \tag{2.2}$$

The operator $\mathcal{F}\left(\sum_{n=0}^{\infty} u_n\right)$ is decomposed in the following recursive form:

$$\mathcal{F}\left(\sum_{n=0}^{\infty} u_n\right) = \mathcal{F}(u_0) + \sum_{n=1}^{\infty}\left[\mathcal{F}\left(\sum_{j=0}^{n} u_j\right) - \mathcal{F}\left(\sum_{j=0}^{n-1} u_j\right)\right] = \sum_{n=1}^{\infty} H_n,$$

where the auxiliary terms are defined by $H_1 = \mathcal{F}(u_0)$ and

$$H_{n+1} = \mathcal{F}\left(\sum_{j=0}^{n} u_j\right) - \mathcal{F}\left(\sum_{j=0}^{n-1} u_j\right), \quad n \geq 1.$$

Substituting the series expression (2.2) into Equation (2.1) leads to a recursive construction:

$$u_0 = \eta, \quad u_n = H_n \quad \text{for } n \geq 1.$$

A finite approximation of the solution using the first p terms is given by

$$u \approx \sum_{n=0}^{p-1} u_n.$$

Uncorrected Proof

Remark 2.4. The decomposition of $\mathcal{F}\big(\sum_{n=0}^{\infty} u_n\big)$ in the display after (2.2) is a telescoping identity. Let $S_n = \sum_{j=0}^{n} u_j$, so that $S_0 = u_0$ and $H_{n+1} = \mathcal{F}(S_n) - \mathcal{F}(S_{n-1})$ for $n \geq 1$. Then, for every $N \geq 1$,

$$\sum_{n=1}^{N+1} H_n = \mathcal{F}(u_0) + \sum_{m=1}^{N}\big[\mathcal{F}(S_m) - \mathcal{F}(S_{m-1})\big] = \mathcal{F}(S_N),$$

hence $\sum_{n=1}^{\infty} H_n = \mathcal{F}(u)$ whenever the series $\sum u_n$ converges to u and $\mathcal{F}$ is continuous at u. No other property of $\mathcal{F}$ is needed; the convergence of $\sum u_n$ is a separate question. For example, for $\mathcal{F}(u) = \ln u$ (defined for $u > 0$) one gets $H_1 = \ln u_0$, $H_{n+1} = \ln(S_n/S_{n-1})$ and $\sum_{n=1}^{N+1} H_n = \ln S_N \to \ln u$, provided $u_0 > 0$, $S_n > 0$ for all n and $u > 0$, i.e. provided all partial sums stay in the domain of $\mathcal{F}$. For the operator $\mathcal{F}(u) = -\varsigma_j u^2$ used in Section 3, $H_{n+1} = -\varsigma_j\,(S_n^2 - S_{n-1}^2)$.

3. The discretized scheme

To numerically approximate the solution of Equation (1.2) over a uniform time grid, we apply the L1 discretization technique for the Caputo fractional derivative and utilize the composite trapezoidal rule for the integral term. Let $M \in \mathbb{N}$ be a fixed positive integer, and define the time step as $\tau = T/M$. The uniform time nodes are then given by $t_j = j\tau$, for $j = 0, 1, \ldots, M$. We denote the numerical approximation of $z(t_j)$ by Z_j. The Caputo fractional derivative $\mathcal{D}_t^\alpha z(t)$ evaluated at t_j, for $j = 1, 2, \ldots, M$, can be expressed as

$$\mathcal{D}_t^\alpha z(t_j) = \frac{1}{\Gamma(1-\alpha)} \sum_{k=0}^{j-1} \int_{s=t_k}^{t_{k+1}} (t_j - s)^{-\alpha} \frac{d}{ds} z(s) ds. \tag{3.1}$$

To approximate the integral term in Equation (3.1), we represent the function $z(t)$ on each subinterval $[t_k, t_{k+1}]$, for $k \geq 0$, using a linear interpolant. Specifically, the interpolation takes the form:

$$z(t) \approx \frac{z(t_{k+1}) - z(t_k)}{\tau} t + \frac{t_{k+1} z(t_k) - t_k z(t_{k+1})}{\tau},$$

where $\tau = t_{k+1} - t_k$ is the constant step size. Differentiating this expression yields

$$\frac{d}{dt} z(t) \approx \frac{1}{\tau} \left[z(t_{k+1}) - z(t_k) \right].$$

Using this linear approximation, the integral in (3.1) can be numerically evaluated following the approach outlined in [4].

$$\begin{aligned} \mathcal{D}_M^\alpha z(t_j) &= \frac{1}{\Gamma(1-\alpha)} \sum_{k=0}^{j-1} \frac{1}{\tau} \big[z(t_{k+1}) - z(t_k) \big] \int_{s=t_k}^{t_{k+1}} (t_j - s)^{-\alpha} ds \\ &= \mu \sum_{k=0}^{j-1} \big[z(t_{k+1}) - z(t_k) \big] \omega_{j-k}, \end{aligned} \tag{3.2}$$

where $\mu = \dfrac{\tau^{-\alpha}}{\Gamma(2-\alpha)}$ and the coefficients are defined as

$$\omega_p = p^{1-\alpha} - (p-1)^{1-\alpha} \text{ for } p = 1(1)M.$$

The truncation error associated with the fractional derivative is given by $R_j^{(1)} = (\mathcal{D}_t^\alpha - \mathcal{D}_M^\alpha) z(t_j)$, where $\mathcal{D}_M^\alpha$ denotes the discrete approximation. For each $j = 1, 2, \ldots, M$, the corresponding integral term can be expressed as

$$I_t z(t_j) = \int_{t_0}^{t_j} z(s) ds = \sum_{k=0}^{j-1} \int_{t_k}^{t_{k+1}} z(s) ds,$$

can be numerically evaluated using the composite trapezoidal rule as follows:

$$I_M z(t_j) = \frac{\tau}{2} \sum_{k=0}^{j-1} \big[z(t_{k+1}) + z(t_k) \big]. \tag{3.3}$$

The remainder is defined by $R_j^{(2)} = (I_t - I_M) z(t_j)$. Using (3.2) and (3.3) the problem (1.2) is transformed to

$$\begin{cases} \mathcal{D}_M^\alpha z(t_j) = a(t_j) z(t_j) - b z^2(t_j) - \lambda z(t_j) I_M z(t_j) + f(t_j) + R_j \text{ for } j = 1(1)M, \\ z(t_0) = z_0, \end{cases} \tag{3.4}$$

where $R_j = R_j^{(1)} + R_j^{(2)}$. Disregarding the remainder term R_j, Equation (3.4) simplifies to:

Uncorrected Proof

$$\begin{cases} \mu \sum_{k=0}^{j-1} \left(Z_{k+1} - Z_k\right) \omega_{j-k} = a_j Z_j - b Z_j^2 - \dfrac{\lambda\tau}{2} Z_j \sum_{k=0}^{j-1} \left[Z_{k+1} + Z_k\right] + f_j \text{ for } j = 1(1)M, \\ Z_0 = z_0. \end{cases} \tag{3.5}$$

Here $f_j = f(t_j)$. Since $\omega_1 = 1$, separating the term $k = j-1$ in the L1 sum and collecting all terms containing Z_j, the scheme (3.5) at time level j is equivalent to the scalar quadratic equation

$$\left(b + \frac{\lambda\tau}{2}\right) Z_j^2 + A_j Z_j = \mu Z_{j-1} + \mu \sum_{k=0}^{j-2} \left(Z_k - Z_{k+1}\right) \omega_{j-k} + f_j, \tag{3.6}$$

where

$$A_j = \mu - a_j + \frac{\lambda\tau}{2} \left[Z_{j-1} + \sum_{k=0}^{j-2} \left(Z_k + Z_{k+1}\right)\right].$$

Dividing (3.6) by A_j (which is positive for τ small, since $\mu = \tau^{-\alpha}/\Gamma(2-\alpha) \to \infty$ as $\tau \to 0$), the approximate solution obtained from scheme (3.5) satisfies the nonlinear implicit algebraic equation

$$u = \eta + \mathcal{F}(u), \tag{3.7}$$

where

$$u = Z_j, \qquad \eta = g^{(j)} := \frac{1}{A_j} \left[\mu Z_{j-1} + \mu \sum_{k=0}^{j-2} \left(Z_k - Z_{k+1}\right) \omega_{j-k} + f_j\right], \qquad \mathcal{F}(u) = \mathcal{F}_j(u) := -\varsigma_j \, u^2,$$

with the scaling factor $\varsigma_j = (b + \lambda\tau/2)/A_j$. Applying the Daftardar–Gejji and Jafari (DGJ) iterative approach of Section 2.2, the terms of the DGJ series at level j are given by the recurrence

$$u_0^{(j)} = g^{(j)}, \quad u_1^{(j)} = \mathcal{F}_j\left(u_0^{(j)}\right) = -\varsigma_j \left(u_0^{(j)}\right)^2, \quad u_{n+1}^{(j)} = \mathcal{F}_j\left(S_n^{(j)}\right) - \mathcal{F}_j\left(S_{n-1}^{(j)}\right) = \varsigma_j \left[\left(S_{n-1}^{(j)}\right)^2 - \left(S_n^{(j)}\right)^2\right], \quad n \geq 1,$$

where $S_n^{(j)} = \sum_{i=0}^{n} u_i^{(j)}$. Therefore, the p-term approximation to the solution of Equation (3.7) is

$$Z_j \approx \sum_{n=0}^{p-1} u_n^{(j)}, \qquad j = 1, 2, \ldots, M.$$

Note that $u_n^{(j)}$ depends on j through $g^{(j)}$ and ς_j. Since $\varsigma_j g^{(j)} = \mathcal{O}(\tau^\alpha)$, Equation (3.7) is a small perturbation of $Z_j = g^{(j)}$ and the DGJ series converges rapidly.

Remark 3.1. At time level t_j ($j = 1, \ldots, M$), evaluating the discretized scheme requires two sums over the history $\{u_k\}_{k=1}^{j-2}$: the L1 (Caputo) convolution $\sum_{k=1}^{j-2} u_k \, \omega_{j-k}$, whose weights ω_{j-k} depend jointly on j and k and therefore cannot be updated recursively – this term costs $O(j)$ operations at level j – and the trapezoidal sum $\sum_{k=1}^{j-2}(u_k + u_{k+1})$, whose summand does not depend on j once k is fixed, so it can be maintained by a single $O(1)$ running update $S_j = S_{j-1} + u_{j-1} + u_j$ instead of being recomputed from scratch at every level. Since the L1 term dominates and costs $O(j)$ at each of the M levels, the total arithmetic cost of the scheme over one time interval is $O(M^2)$, with $O(M)$ storage for $\{u_j\}_{j=1}^{M}$. Table 2 reports the measured CPU time of the (recursively-updated) implementation for Example 5.1, for $M = 32, \ldots, 2048$ and several values of α; the CPU time increases with M for every α tested, consistent with this $O(M^2)$ operation count.

Uncorrected Proof

4. Error estimation

Lemma 4.1. *Let $z(t) \in C^2[0,T]$, then $\left|R_j^{(1)}\right| \leq C\tau^{(2-\alpha)}$ for $j = 1, 2, \ldots, M$.*

Proof. Using definition

$$\begin{aligned}\left|R_j^{(1)}\right| &= \left|(\mathcal{D}_t^\alpha - \mathcal{D}_M^\alpha) z(t_j)\right| \\ &= \left|\frac{1}{\Gamma(1-\alpha)} \sum_{k=0}^{j-1} \int_{s=t_k}^{t_{k+1}} (t_j - s)^{-\alpha} \left[z'(s) - \frac{z(t_{k+1}) - z(t_k)}{\tau}\right] ds\right| \\ &\leq C\left|\frac{1}{\Gamma(1-\alpha)} \sum_{k=0}^{j-1} \int_{s=t_k}^{t_{k+1}} \frac{t_j + t_{j-1} - 2s}{(t_j - s)^\alpha} ds + \mathcal{O}(\tau^2)\right|.\end{aligned}$$

From [8], we get $\left|\frac{1}{\Gamma(1-\alpha)} \sum_{k=0}^{j-1} \int_{s=t_k}^{t_{k+1}} \frac{t_j + t_{j-1} - 2s}{(t_j - s)^\alpha} ds\right| \leq C\tau^{(2-\alpha)}$. This however means $|R_j^{(1)}| \leq C\tau^{(2-\alpha)}$. Hence completes the proof. □

Lemma 4.2. *Assume that $z(t) \in C^2[0,T]$. Then, the error associated with the composite rule applied in equation (3.3) can be bounded by the following estimate:*

$$|R_j^{(2)}| \leq CT\tau^2.$$

Proof. Since $z(t) \in C^2[0,T]$, $\exists$ positive constant C_1 such that $|z^{(i)}(t)| \leq C_1$ for $i = 0, 1, 2$. Now, we have

$$\begin{aligned}\left|R_j^{(2)}\right| &= \left|(I_t - I_M) z(t_j)\right| \\ &= \frac{t_j \tau^2}{12} \max_{0 \leq s \leq t_j} \left|\frac{\partial^2 z}{\partial s^2}(s)\right| \\ &\leq \frac{j\tau^3}{12} C_1 \leq \frac{M\tau^3}{12} C_1 \leq CT\tau^2,\end{aligned}$$

which represents the required error bound. □

Let the error at each time level $j = 1, 2, \ldots, M$ be denoted by $e_j = z(t_j) - Z_j$. By substituting Equation (3.5) into (3.4), we obtain:

$$\begin{cases} \mathcal{D}_M^\alpha e_j = a_j e_j - b(z^2(t_j) - Z_j^2) - \dfrac{\lambda\tau}{2} \sum_{k=0}^{j-1} \big(K(t_j, z(t_k)) - K(t_j, Z_k) \\ \qquad\qquad + K(t_j, z(t_{k+1})) - K(t_j, Z_{k+1})\big), \qquad \text{for} \quad j = 1(1)M, \\ e_0 = 0, \end{cases} \tag{4.1}$$

Given that $K(t, z(s)) = z(t)z(s)$, and both $z^2(t)$ and the kernel K exhibit Lipschitz continuity, there exist positive constants M_1 and M_2 such that Equation (4.1) can be reformulated as:

$$\begin{cases} \mathcal{D}_M^\alpha |e_j| \leq |a_j||e_j| + L_1|e_j| + \dfrac{\lambda L_2 \tau}{2} \sum_{k=0}^{j-1} \big(|e_k| + |e_{k+1}|\big) + R_j \text{ for } j = 1(1)M, \\ e_0 = 0. \end{cases} \tag{4.2}$$

Theorem 4.3. *Let $z \in C^2[0,T]$ be the exact solution of (1.2) and let $\{Z_j\}_{j=1}^M$ be the solution of the discrete scheme (3.5). Then there exists $\tau_0 > 0$, determined by $(\max_j |a_j| + L_1)\,\Gamma(2-\alpha)\,\tau_0^\alpha < 1$, such that for all $\tau \leq \tau_0$ the following relation holds:*

$$\max_{1 \leq j \leq M} \left|z(t_j) - Z_j\right| \leq C\tau^{(2-\alpha)}.$$

Uncorrected Proof

Proof. Given that $e_0 = 0$, and applying Equation (3.2), inequality (4.2) can be reformulated as:

$$\mu\Big\{|e_j| - \sum_{k=1}^{j-1} \left(\omega_k - \omega_{k+1}\right) |e_{j-k}|\Big\} \leq (|a_j| + L_1)|e_j| + \lambda L_2 \tau \sum_{k=1}^{j-1} |e_k| + |R_j|,$$

By simplifying, we get

$$|e_j| \leq \frac{L_3}{\mu - (|a_j| + L_1)} \sum_{k=1}^{j-1} |e_k| + \frac{1}{\mu - (|a_j| + L_1)} |R_j|,$$

where $L_3 = \max_{1\leq k\leq j-1} \Big\{\mu\big(\omega_{j-k} - \omega_{j-k+1}\big) + \lambda L_2 \tau\Big\}$. From [9] for $\dfrac{|a_j| + L_1}{\mu} < 1$ and if $\lim_{\tau\to 0} \sum_{k=1}^{j-1} |e_k| = 0$, we have

$$|e_j| \leq L_3 \exp\Big(\frac{1}{\mu - (|a_j| + L_1)}\Big) \sup_{0\leq k\leq j} \Big\{\frac{|R_k|}{\mu - (|a_j| + L_1)}\Big\}. \tag{4.3}$$

Utilizing Lemmas 4.1 and 4.2, we obtain the following result:

$$|R_j| \leq |R_j^{(1)}| + |R_j^{(2)}| \leq C\big(\tau^{(2-\alpha)} + \tau^2\big). \tag{4.4}$$

Hence, by using (4.4), the relation (4.3) yields

$$\max_{1\leq j\leq M} |e_j| \leq L_3 \exp\Big(\frac{1}{\mu - (|a_j| + L_1)}\Big) \sup_{0\leq k\leq j} \Big\{\frac{C\big(\tau^{(2-\alpha)} + \tau^2\big)}{\mu - (|a_j| + L_1)}\Big\} \leq C\tau^{(2-\alpha)}.$$

This completes the proof of the theorem. □

5. Numerical examples

In this section we provide some numerical experiments in order to asses accuracy of proposed method. All computations and numerical experiments reported in this study were performed using MATLAB R2025b.

Example 5.1. Consider the following test example:

$$\begin{cases} \mathcal{D}_t^{\alpha} z(t) = e^t z(t) - z^2(t) - z(t) \int_0^t z(s)\, ds + f(t), \quad t \in (0, 1], \\ z(0) = 1. \end{cases}$$

Select the source function $f(t)$ such that the exact solution is given by $z(t) = t^{2+\alpha}+1$. The maximum error is computed using the formula $\Sigma_M = \max_{0\leq j\leq M} |z(t_j) - Z_j|$, and the convergence rate is determined by $\varrho_M = \log_2\left(\dfrac{\Sigma_M}{\Sigma_{2M}}\right)$, so that ϱ_M needs the error on the next finer mesh. Figure 1 illustrates the exact and numerical solutions corresponding to Example 5.1, demonstrating that the numerical approximation improves and closely follows the exact solution as the grid is refined. Figure 2 displays the numerical solutions obtained for various values of α. It can be observed that as α approaches 1, the computed solutions tend to align more closely with the classical (non-fractional) solution. In Figure 3, log-log plots illustrate the behavior of the absolute error for $\alpha = 0.3$ and $\alpha = 0.7$. The corresponding values of the maximum error Σ_M and the estimated convergence rates ϱ_M are listed in Table 1. These results clearly confirm that the proposed scheme achieves convergence to the exact solution with a desirable level of accuracy. Table 2 reports the CPU time, in seconds, required to compute the numerical solution for each α and each mesh size N up to 2048. Moreover one can observe that rates agree with the theoretical order $2-\alpha$ of Theorem 4.3. The error at a fixed mesh increases with α, in agreement with the estimate $C\tau^{2-\alpha}$, for two reasons. First, since $\tau < 1$, the factor $\tau^{2-\alpha}$ increases with α: for $M = 32$ it equals about 1.9×10^{-3} for $\alpha = 0.2$ and 2.2×10^{-2} for $\alpha = 0.9$. Second, the constant C also grows with α, because it contains $\|z''\|_\infty$ and the constant of the L1 truncation error; here $z''(t) = (2+\alpha)(1+\alpha)t^{\alpha}$, whose maximum on $[0, 1]$ grows from 2.64 ($\alpha = 0.2$) to 5.51 ($\alpha = 0.9$). As $\alpha \to 1^-$ the L1 formula reduces to the backward Euler difference, which is first-order accurate; the rates $\varrho_M \approx 1.1$ for $\alpha = 0.9$ reflect this.

Uncorrected Proof

In the next two examples we use the model of Example 5.1, i.e. $\mathcal{D}_t^\alpha z = e^t z - z^2 - z\int_0^t z(s)\,ds + f(t)$, $t \in (0,1]$, $z(0) = 1$, with the source function f chosen so that the exact solution is not a polynomial.

Example 5.2. Let the exact solution be $z(t) = e^t$. The source function is $f(t) = t^{1-\alpha}E_{1,2-\alpha}(t) + e^{2t} - e^t$, where $E_{\beta,\gamma}$ is the Mittag-Leffler function (2.3).

Table 3 reports the maximum errors and the rates of convergence for this smooth solution. As M increases the observed rates steadily approach the theoretical order $2-\alpha$ of Theorem 4.3 (e.g. 1.67, 1.49, 1.30, 1.10 for $\alpha = 0.3$, 0.5, 0.7, 0.9 between $M = 1024$ and $M = 2048$), and the rate decreases as α increases toward 1, consistent with the order $2-\alpha$ deteriorating to first order (backward Euler) in that limit. This confirms the theoretical error estimate for a solution satisfying the regularity hypotheses of Theorem 4.3.

Example 5.3. (Weakly singular solution.) Let the exact solution be the Mittag-Leffler function $z(t) = E_{\alpha,1}(-t^\alpha)$. The source function is

$$f(t) = -z(t) - e^t z(t) + z^2(t) + t\,z(t)\,E_{\alpha,2}(-t^\alpha).$$

Here $z'(t) \sim t^{\alpha-1}$ is unbounded at $t = 0$, so $z \notin C^2[0,1]$ and the hypotheses of Theorem 4.3 are not satisfied.

Table 4 shows that the scheme still converges for this weakly singular solution, but at a visibly reduced rate: on the uniform mesh the observed order is close to α itself, rather than the $2-\alpha$ seen in Example 5.2. This drop in accuracy is a direct consequence of the unbounded derivative $z'(t) \sim t^{\alpha-1}$ at $t = 0$, which places the solution outside the smoothness assumptions of Theorem 4.3; it illustrates, on a worked example, the loss of accuracy near a weak singularity discussed in Remark 5.5, and points to the need for a graded mesh near $t = 0$ if the full order $2-\alpha$ is to be recovered for such solutions.

Example 5.4. Consider the classical dimensionless form of Volterra's population model of fractional order [6],

$$\kappa\,\mathcal{D}_t^\alpha z(t) = z(t) - z^2(t) - z(t)\int_0^t z(s)\,ds, \qquad z(0) = 0.1,$$

which is (1.2) with $a(t) = b = \lambda = 1/\kappa$ and $f \equiv 0$; here $\kappa = \lambda/(ab)$ is the dimensionless toxicity parameter. This is the benchmark used in the literature on this model, with $\kappa \in \{0.02, 0.04, 0.1, 0.2, 0.5\}$.

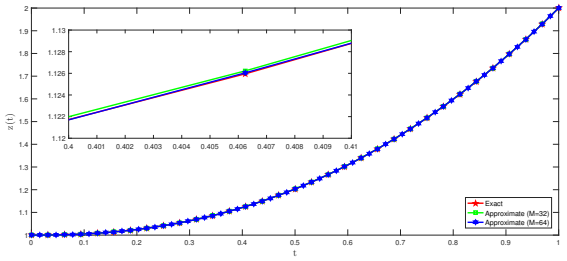
No closed-form solution is available for fractional α, and for $\alpha = 1$ the classical solution is known through its maximum value $z_{\max}$ [24]. We compute $z_{\max}$ and the time $t_{\max}$ at which it is attained, on $[0,T]$ with $T = 3$. Table 5 compares the values for $\alpha = 1$ with the exact values [24] and with the numerical values reported independently by [6] and by [25], on the meshes $M = 2^{13}$ and $M = 2^{14}$. Since no exact solution or comparable published $z_{\max}$ values are available for fractional α, Table 6 assesses accuracy there by the same double-mesh principle: $z_{\max}$ and $t_{\max}$ are computed on both $M = 2^{13}$ and $M = 2^{14}$ for $\alpha = 3/4$ and $\alpha = 1/2$, and the double-mesh estimate $\Delta_M = |z_{\max}^{2M} - z_{\max}^{M}|$ is reported alongside the finer-mesh values; Δ_M is of order 10^{-5}–10^{-6} across all κ, confirming convergence in the fractional case as well.

Here, we summarize some key features and limitations of the proposed scheme.

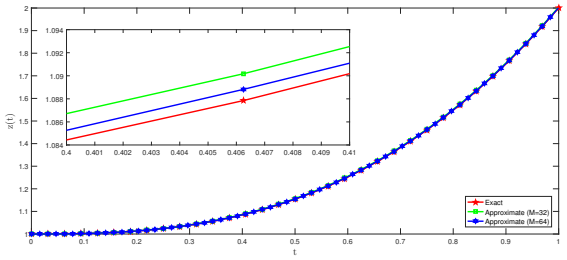
Remark 5.5 (Key features of the scheme)**.** *Properties.* (a) The scheme is a time-marching scheme: level j needs only the history $Z_0, \ldots, Z_{j-1}$ and the solution of the scalar equation (3.7), so no global nonlinear system, Jacobian or starting guess is required. (b) It combines the L1 formula on a uniform mesh, the composite trapezoidal rule and the DGJ iteration; the truncation error is $\mathcal{O}(\tau^{2-\alpha} + \tau^2)$ for $z \in C^2[0,T]$ and the scheme converges with order $2-\alpha$ in the maximum norm (Theorem 4.3). (c) The cost is $\mathcal{O}(M^2)$ operations, driven by the L1 history sum, and $\mathcal{O}(M)$ storage (Remark 3.1); this is confirmed empirically by the observed CPU-time scaling. (d) Variable growth rates $a(t)$ and source terms $f(t)$ are handled without change.

Weaknesses. (a) The convergence order $2-\alpha$ deteriorates to first order as $\alpha \to 1$, since the L1 approximation reduces to the backward Euler difference in this limiting case. (b) The error analysis requires $z \in C^2[0,T]$. For solutions exhibiting a weak singularity at $t = 0$, which is common in fractional differential equations, the use of a uniform mesh may fail to adequately resolve the initial layer, resulting in a deterioration of the observed convergence rate. In such cases, graded meshes or suitable correction terms may be required to recover the optimal convergence

Uncorrected Proof



(A) $\alpha = 0.3$.



(B) $\alpha = 0.7$.

FIGURE 1. Comparison between the exact and numerical solutions for different mesh resolutions corresponding to Example 5.1.

Uncorrected Proof

rate. In Example 5.3, the exact solution possesses a weak singularity at $t = 0$, and the numerical results demonstrate the corresponding deterioration in the convergence rate. (c) The $\mathcal{O}(M^2)$ cost of the L1 history term is inherent to the scheme and is not reduced by mesh refinement; fast evaluation techniques (e.g. sum-of-exponentials kernel approximations) would be needed to lower it for very fine meshes.

6. CONCLUSION

This study presents an iterative finite difference method for a fractional-order population dynamics model of Volterra type. The method combines the L1 approximation of the Caputo derivative on a uniform mesh with the composite trapezoidal rule for the integral term; at each time level the resulting nonlinear equation is a scalar quadratic equation, which is solved by the Daftardar–Gejji and Jafari (DGJ) iteration. It was proved that, for $z \in C^2[0, T]$ and τ sufficiently small, the scheme converges in the maximum norm with order $(2 - \alpha)$.

We performed extensive numerical experiments on a range of test problems, including problems with known smooth and weakly singular exact solutions as well as a benchmark comparison example from the literature, and observed good accuracy throughout: the theoretical convergence order is closely reproduced for smooth solutions, while the scheme remains reliable, with reduced but consistent accuracy, for solutions with weaker regularity.

The main limitations of the method are the deterioration of the order as $\alpha \to 1$, the reduced rate for solutions with a weak initial singularity on uniform meshes, and the quadratic cost of the L1 history term. Future work includes graded meshes to recover the full rate for weakly singular solutions, fast evaluation of the history term, higher-order approximations of the fractional derivative, and the error analysis of the DGJ truncation.

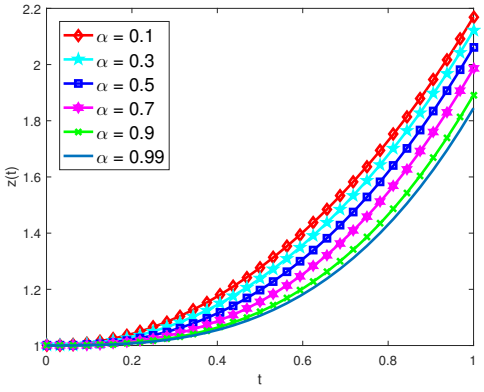
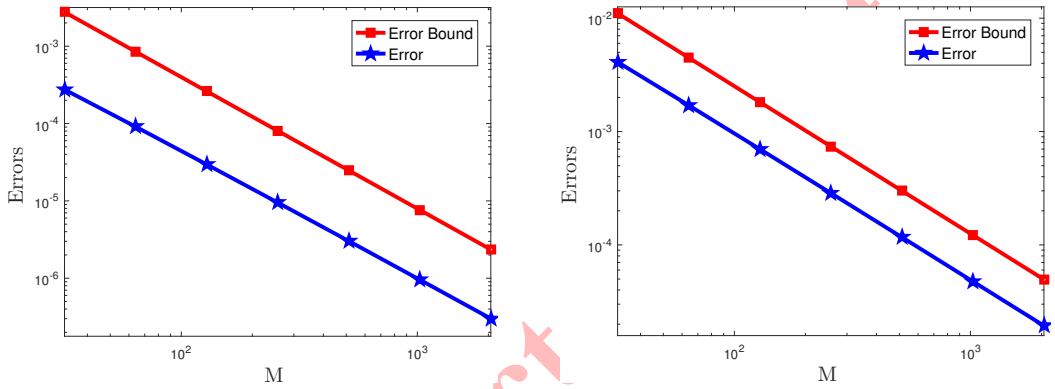


FIGURE 2. Numerical solutions for various values of α with fixed mesh size $M = 32$ for Example 5.1.



(A) $\alpha = 0.3$. (B) $\alpha = 0.7$.

FIGURE 3. Log–log plots of the maximum error Σ_M for Example 5.1.

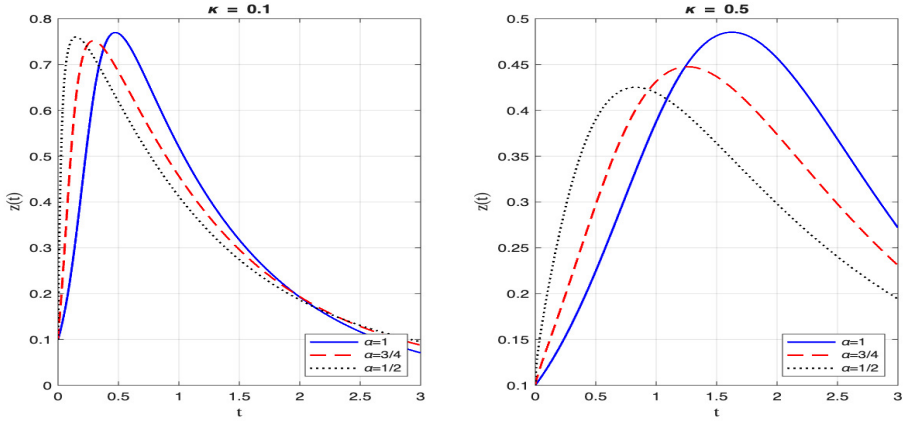


FIGURE 4. Solution profiles $z(t)$ of the population model for $\alpha = 1, 3/4, 1/2$ at $\kappa = 0.1$ (left) and $\kappa = 0.5$ (right): decreasing α advances the peak time and lowers the peak amplitude for Example 5.4.

TABLE 1. Maximum absolute errors Σ_M and corresponding convergence rates ϱ_M for Example 5.1. The rate $\varrho_M = \log_2(\Sigma_M/\Sigma_{2M})$ is listed under M.

α/M	32	64	128	256	512	1024	2048	4096
0.2	1.144E-04	3.653E-05	1.140E-05	3.503E-06	1.064E-06	3.216E-07	9.641E-08	2.825E-08
ϱ_M	1.647	1.680	1.703	1.719	1.726	1.738	1.771	–
0.3	2.750E-04	9.108E-05	2.963E-05	9.516E-06	3.028E-06	9.567E-07	3.008E-07	9.403E-08
ϱ_M	1.594	1.620	1.639	1.652	1.662	1.669	1.678	–
0.4	5.808E-04	2.018E-04	6.907E-05	2.340E-05	7.873E-06	2.636E-06	8.790E-07	2.923E-07
ϱ_M	1.525	1.547	1.561	1.572	1.579	1.584	1.588	–
0.6	2.201E-03	8.578E-04	3.307E-04	1.267E-04	4.832E-05	1.839E-05	6.989E-06	2.653E-06
ϱ_M	1.359	1.375	1.384	1.390	1.394	1.396	1.397	–
0.8	7.510E-03	3.333E-03	1.466E-03	6.415E-04	2.800E-04	1.221E-04	5.318E-05	2.316E-05
ϱ_M	1.172	1.185	1.192	1.196	1.198	1.199	1.199	–
0.9	1.353E-02	6.428E-03	3.027E-03	1.419E-03	6.634E-04	3.099E-04	1.446E-04	6.750E-05
ϱ_M	1.073	1.087	1.093	1.097	1.098	1.099	1.099	–

TABLE 2. CPU time (in seconds) of Table 1 for Example 5.1.

$\alpha\backslash M$	32	64	128	256	512	1024	2048
0.2	0.000047	0.000063	0.000132	0.000294	0.000707	0.001910	0.005779
0.3	0.000032	0.000063	0.000137	0.000296	0.000710	0.001907	0.005786
0.4	0.000032	0.000063	0.000132	0.000293	0.000710	0.001913	0.005784
0.6	0.000032	0.000063	0.000132	0.000293	0.000710	0.001907	0.005844
0.8	0.000032	0.000063	0.000132	0.000293	0.000707	0.001908	0.005778
0.9	0.000031	0.000063	0.000132	0.000296	0.000738	0.001910	0.005793

TABLE 3. Maximum absolute errors Σ_M and convergence rates ϱ_M for Example 5.2.

α/M	32	64	128	256	512	1024	2048
0.3	1.311E-04	4.360E-05	1.422E-05	4.576E-06	1.458E-06	4.611E-07	1.450E-07
ϱ_M	1.589	1.616	1.636	1.650	1.661	1.669	–
0.5	4.849E-04	1.783E-04	6.472E-05	2.329E-05	8.336E-06	2.972E-06	1.057E-06
ϱ_M	1.443	1.462	1.474	1.482	1.488	1.491	–
0.7	1.515E-03	6.286E-04	2.585E-04	1.057E-04	4.312E-05	1.756E-05	7.141E-06
ϱ_M	1.269	1.282	1.290	1.294	1.296	1.298	–
0.9	4.402E-03	2.086E-03	9.809E-04	4.594E-04	2.148E-04	1.003E-04	4.682E-05
ϱ_M	1.077	1.089	1.094	1.097	1.099	1.099	–

Uncorrected Proof

TABLE 4. Maximum absolute errors Σ_M and convergence rates ϱ_M for Example 5.3 (weakly singular solution).

α/M	32	64	128	256	512	1024	2048
0.3	5.199E-02	4.430E-02	3.750E-02	3.159E-02	2.650E-02	2.213E-02	1.842E-02
ϱ_M	0.231	0.240	0.247	0.254	0.260	0.265	–
0.5	3.789E-02	2.762E-02	2.000E-02	1.440E-02	1.032E-02	7.371E-03	5.251E-03
ϱ_M	0.456	0.466	0.474	0.480	0.485	0.489	–
0.7	1.797E-02	1.106E-02	6.804E-03	4.188E-03	2.578E-03	1.587E-03	9.766E-04
ϱ_M	0.701	0.701	0.700	0.700	0.700	0.700	–
0.9	1.348E-02	6.703E-03	3.332E-03	1.656E-03	8.234E-04	4.094E-04	2.036E-04
ϱ_M	1.008	1.008	1.008	1.008	1.008	1.008	–

TABLE 5. Maximum population $z_{\max}$ for $\alpha = 1$ in Example 5.4.

κ	Exact [24]	[6]	[25]	Present, $M = 2^{13}$	Present, $M = 2^{14}$
0.02	0.92342717	0.922942037	0.90383805	0.923045	0.923236
0.04	0.87371998	0.873725344	0.86124018	0.873446	0.873583
0.1	0.76974149	0.765113089	0.76511308	0.769588	0.769665
0.2	0.65905038	0.659050432	0.65791231	0.658964	0.659007
0.5	0.48519030	0.485190290	0.48528235	0.485156	0.485173

TABLE 6. Maximum population $z_{\max}$ and time $t_{\max}$ of its occurrence for fractional α in Example 5.4, with the double-mesh estimate $\Delta_M = |z_{\max}^{2M} - z_{\max}^{M}|$ $(M = 2^{13})$.

	$\alpha = 3/4$			$\alpha = 1/2$		
κ	$z_{\max}$	$t_{\max}$	Δ_M	$z_{\max}$	$t_{\max}$	Δ_M
0.02	0.90365	0.0691	2.14E-05	0.91377	0.0356	6.90E-06
0.04	0.85497	0.1261	2.32E-05	0.86520	0.0632	8.11E-06
0.1	0.75168	0.2919	1.93E-05	0.76011	0.1488	9.12E-06
0.2	0.63627	0.5562	1.39E-05	0.63758	0.3074	8.42E-06
0.5	0.44756	1.2581	7.56E-06	0.42510	0.8284	5.81E-06

Uncorrected Proof

Conflict of Interest

Authors have no conflict of interest.

Data Availability Statement

All data is included within the manuscript.

Acknowledgment

The fourth author acknowledges the Department of Science and Technology (DST), Government of India, for providing infrastructural support to the Department of Mathematics, NIT Rourkela, under the DST-FIST programme through Grant No. SR/FST/MS-I/2021/103(C).

References

[1] E. Ahmed and A. S. Elgazzar, *On fractional order differential equations model for nonlocal epidemics*, Phys. A: Stat. Mech. Appl., *379*(2) (2007), 607–614.
[2] D. Baleanu, B. Agheli, M. Adabitabar Firozja, and M. M. Al Qurashi, *A method for solving nonlinear Volterra's population growth model of noninteger order*, Adv. Differ. Equ., *2017* (2017), 1–8.
[3] V. Daftardar-Gejji and H. Jafari, *An iterative method for solving nonlinear functional equations*, J. Math. Anal. Appl., *316*(2) (2006), 753–763.
[4] B. Ghosh and J. Mohapatra, *Analysis of finite difference schemes for Volterra integro-differential equations involving arbitrary order derivatives*, J. Appl. Math. Comput., *69*(2) (2023), 1865–1886.
[5] S. Kazemi and A. Tari, *Convergence analysis of the collocation method for solving two-dimensional fractional Volterra integro-differential equations*, Iran. J. Sci., *48*(6) (2024), 1515–1527.
[6] N. A. Khan, A. Ara, and M. Jamil, *Approximations of the nonlinear Volterra's population model by an efficient numerical method*, Math. Methods Appl. Sci., *34*(14) (2011), 1733–1738.
[7] K. Krishnarajulu, K. Krithivasan, and R. B. Sevugan, *Fractional polynomial method for solving fractional order population growth model*, Commun. Korean Math. Soc., *31*(4) (2016), 869–878.
[8] Y. Lin and C. Xu, *Finite difference/spectral approximations for the time-fractional diffusion equation*, J. Comput. Phys., *225*(2) (2007), 1533–1552.
[9] P. Linz, *Analytical and Numerical Methods for Volterra Equations*, SIAM Publications, Philadelphia, 1985.
[10] M. Maleki and M.T. Kajani, *Numerical approximations for Volterra's population growth model with fractional order via a multi-domain pseudospectral method*, Appl. Math. Model., *39*(15) (2015), 4300–4308.
[11] H. R. Marzban, S.M. Hoseini, and M. Razzaghi, *Solution of Volterra's population model via block-pulse functions and Lagrange-interpolating polynomials*, Math. Methods Appl. Sci., *32*(2) (2009), 127–134.
[12] F. Mirzaee, S. Bimesl and E. Tohidi, *Solving nonlinear fractional integro-differential equations of Volterra type using novel mathematical matrices*, J. Comput. Nonlinear Dyn., *10*(6) (2015), 061016.
[13] F. Mirzaee and S.F. Hoseini, *A new collocation approach for solving systems of high-order linear Volterra integro-differential equations with variable coefficients*, Appl. Math. Comput., *311* (2017), 272–282.
[14] F. Mirzaee, E. Solhi, and S. Naserifar, *Approximate solution of stochastic Volterra integro-differential equations by using moving least squares scheme and spectral collocation method*, Appl. Math. Comput., *410* (2021), 126447.
[15] M. Mojahedfar and A. Tari Marzabad, *Solving two-dimensional fractional integro-differential equations by Legendre wavelets*, Bull. Iran. Math. Soc., *43*(7) (2017), 2419–2435.
[16] K. Parand, Z. Delafkar, N. Pakniat, A. Pirkhedri, and M. Kazemnasab Haji, *Collocation method using sinc and Rational Legendre functions for solving Volterra's population model*, Commun. Nonlinear Sci. Numer. Simul., *16*(4) (2011), 1811–1819.
[17] K. Parand and M. Delkhosh, *Solving Volterra's population growth model of arbitrary order using the generalized fractional order of the Chebyshev functions*, Ric. Mat., *65* (2016), 307–328.
[18] I. Podlubny, *Fractional Differential Equations*, Mathematics in Science and Engineering, Vol. 198, Academic Press, San Diego, 1998.

Uncorrected Proof

[19] L. Saeedi, A. Tari, and S. H. Momeni Masuleh, *Numerical solution of a class of the nonlinear Volterra integro-differential equations*, J. Appl. Math. Inform., *31* (2013), 65–77.
[20] F. M. Scudo, *Vito Volterra and theoretical ecology*, Theor. Popul. Biol., *2* (1971), 1–23.
[21] F. A. Shah, M. Irfan, and K. S. Nisar, *Gegenbauer wavelet quasi-linearization method for solving fractional population growth model in a closed system*, Math. Methods Appl. Sci., *45*(7) (2022), 3605–3623.
[22] V. E. Tarasov, *Fractional Dynamics: Application of Fractional Calculus to Dynamics of Particles, Fields and Media*, Springer Science and Business Media, 2010.
[23] A. Tari and S. Shahmorad, *A computational method for solving two-dimensional linear Volterra integral equations of the first kind*, Scientia Iranica D, *19*(3) (2012), 829–835.
[24] K. G. TeBeest, *Numerical and analytical solutions of Volterra's population model*, SIAM Rev., *39*(3) (1997), 484–493.
[25] A. M. Wazwaz, *Analytical approximations and Padé approximants for Volterra's population model*, Appl. Math. Comput., *100* (1999), 13–25.
[26] M. Williamson, *The Analysis of Biological Populations*, Edward Arnold, London, 1972.
[27] H. Xu, *Analytical approximations for a population growth model with fractional order*, Commun. Nonlinear Sci. Numer. Simul., *14*(5) (2009), 1978–1983.

Uncorrected Proof